CONF-9710153--

LA-UR-97-4201

Title: CHARACTERIZATION OF PLASMA SPRAYED BERYLLIUM ITER FIRST WALL MOCKUPS

Author(s): RICHARD G. CASTRO, MST-6
RAJENDRA U. VAIDYA, MST-6
KENDALL J. HOLLIS, MST-6

Submitted to: 3RD IEA INTERNATIONAL WORKSHOP ON BERYLLIUM TECHNOLOGY FOR FUSION TO BE HELD AT MITO, JAPAN ON OCTOBER 22-24, 1997

Los Alamos
NATIONAL LABORATORY

DISCLAIMER

Characterization of Plasma Sprayed Beryllium ITER First Wall Mockups

R.G. Castro[a], R.U. Vaidya[a], and K.J. Hollis[a]

[a]Los Alamos National Laboratory, Material Science and Technology Division
P.O. Box 1663, Mail Stop G770,Los Alamos, New Mexico 87545, USA

ITER first wall beryllium mockups, which were fabricated by vacuum plasma spraying the beryllium armor, have survived 3000 thermal fatigue cycles at 1 MW/m^2 without damage during high heat flux testing at the Plasma Materials Test Facility at Sandia National Laboratory in New Mexico. The thermal and mechanical properties of the plasma sprayed beryllium armor have been characterized. Results are reported on the chemical composition of the beryllium armor in the as-deposited condition, the through thickness and normal to the through thickness thermal conductivity and thermal expansion, the four-point bend flexure strength and edge-notch fracture toughness of the beryllium armor, the bond strength between the beryllium armor and the underlying heat sink material, and ultrasonic C-scans of the Be/heat sink interface.

1. INTRODUCTION

Investigations are being conducted within the International Thermonuclear Experimental Reactor (ITER) community to qualify a process for joining beryllium armor directly to an actively cooled copper heat sink for the primary first wall. A number of joining techniques are currently being evaluated by the international ITER community which include silverless brazing, diffusion bonding, hot isostatic press (HIPing) bonding, explosive bonding and plasma spraying [1]. In all cases joining beryllium directly to copper presents a challenging problem due to the formation of brittle intermetallic compounds (*e.g.* BeCu, Be_2Cu) at the interface. Plasma spraying is being investigated due to its flexibility of providing thick coatings of beryllium directly on large flat and curved copper surfaces on the primary first wall of ITER. In an initial study, Be/Cu mockups produced by plasma spraying survived 3000 thermal fatigue cycles at 1 MW/m^2 without damage during testing at the Plasma Materials Test Facility at Sandia National Laboratories [2]. This heat flux was twice the expected design heat flux for the first wall modules in ITER. Results of this test demonstrated the viability of plasma spraying as a method for fabricating the beryllium first wall armor for ITER.

In this investigation the thermal and mechanical properties of the plasma sprayed beryllium armor on the Be/Cu mockups were evaluated. Specific properties which were characterized included the through thickness and normal to the through thickness thermal conductivity and thermal expansion, the four-point bend flexure strength and edge-notch fracture toughness, and interfacial bond strength between the beryllium armor and the heat sink material. Chemical analysis of the beryllium armor after plasma spraying was also evaluated and compared to the initial powder feedstock material composition.

2. EXPERIMENTAL

Two Be/Cu mockups were vacuum plasma sprayed by translating the plasma sprayed torch in an X and Y motion over the surface of the copper heat sink and stainless steel fixturing while simultaneously depositing beryllium, Fig 1. Thick beryllium coatings (> 15mm) were deposited on the surface of two different types of copper heat sinks: 1) a CuNiBe heat sink and 2) a CuCrZr heat sink which had aluminum explosively bonded to the surface with a thin titanium diffusion barrier interlayer between copper and aluminum. Subsequent machining and profiling of the beryllium armor on the heat sinks was done in order to provide 5 and 10 mm thick individual beryllium tiles for the high heat flux testing. Details on the fabrication, machining and high heat flux testing of the plasma sprayed Be/Cu mockups can be found in reference [2].

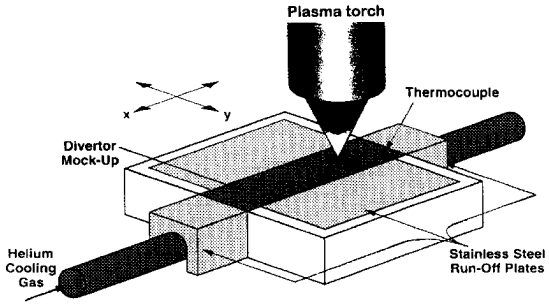

Fig. 1. Schematic of the translation of the plasma spray torch to produce the Be/Cu plasma sprayed mockups.

To characterize the thermal and mechanical properties of the plasma sprayed beryllium, test samples were machined directly from the thick beryllium armor.

2.1 Mechanical Properties

2.1.1. Flexure strength and fracture toughness

To evaluate the mechanical properties of the beryllium plasma sprayed armor, four-point bend flexure strength and single-edge notched fracture toughness testing (in four-point bending) were performed, Fig. 2.

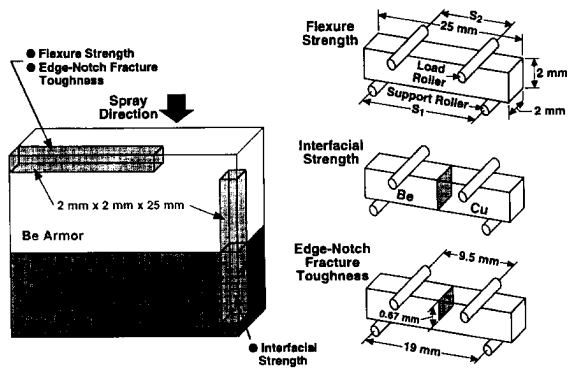

Fig.2. Schematic showing the sample dimensions and orientation of the 4-point bend flexure strength, interfacial strength and edge-notch fracture toughness samples.

The four-point bend samples were electro-discharge machined (EDM) from the beryllium armor. The sample dimensions were 25 mm long x 2 mm wide x 2 mm thick. Each sample was polished to a 600 grit finish on all four sides before testing. The samples were tested in an Instron machine using a cross-head speed of 0.1 mm/min. An outer support span of 19 mm coupled with an inner loading span of 9.5 mm was used on all of the bend tests. Fracture toughness measurements were carried out using a single-edge notched beam specimen. Notches in the four-point bend samples were cut to one-third of the sample thickness (0.67 mm) using a slow speed diamond saw. A total of five samples were used to obtain the average value for both the flexure strength and the single-edge notched fracture toughness. The four-point bend flexure strength tests were carried out in accordance with ASTM standard C-203/85. The fracture toughness tests were carried out in accordance with ASTM standard STP 678.

2.1.2. Interfacial strength and adhesion

To determine the interfacial strength of the plasma sprayed beryllium armor on the CuNiBe heat sink and the CuCrZr heat sink with the explosive bonded aluminum layer, four-point bend testing was also performed. The samples tested were 25 mm long x 2 mm wide x 2 mm thick. The interface was located at the center of the sample (12.5 mm from the edge) within the inner loading span, Fig. 2. The four-point bend interfacial strength tests were performed under the same loading conditions used for the flexure strength and fracture toughness tests. The samples were all taken to failure during testing. Characterization of the interface between the beryllium plasma sprayed armor and the heat sink material was performed using scanning electron microscopy. A non-destructive evaluation using C-scan ultrasonics was also performed on the Be/Cu mockups to qualitatively determine the integrity of the bond between the beryllium plasma sprayed armor and the underlying heat sink. In performing the ultrasonic test, the energy level of the ultrasonic transmitter, the attenuation of the ultrasonic receiver and the relative location of the probe to the specimen were adjusted to give a good contrast between a relatively good and a bad bond at the interface. The NDE tests were performed at KARTA Technology using a Krauthramer HIS-1 ultrasonic analyzer with an attenuation of 39dB. A 5 and 10 Mhz probe with a .25 inch diameter

piezoelectric crystal (Panametrics V312) was used on all scans.

2.2 Thermal Properties

2.2.1. Thermal conductivity and expansion

Thermal diffusivity samples (3 mm thick x 12.7 mm in diameter) and thermal expansion samples (5 mm in diameter x 8 mm long) were machined from scrap material after the beryllium armor had been machined to the required dimensions. To evaluate the microstructural effects on the thermal properties of the plasma sprayed armor, samples were machined from two different orientations; 1) through the thickness of the beryllium armor coating (i.e., in the sprayed direction) and 2) in the plane of the coating (i.e., normal to the spray direction), Fig 3.

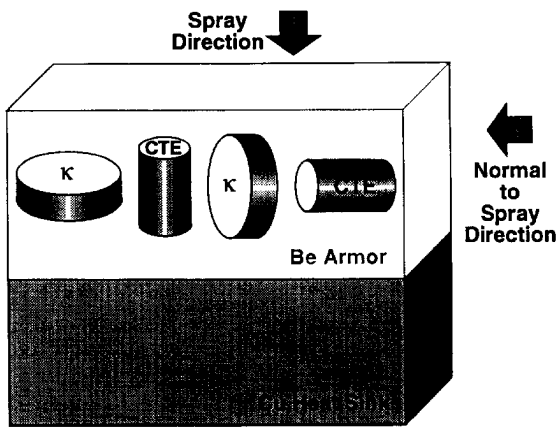

Fig 3. Schematic showing the sample dimensions and orientation of the thermal expansion and thermal conductivity tests samples.

Thermal diffusivity measurements were performed at Virginia Polytechnic University using a laser flash diffusivity technique [3]. The thermal conductivity of the beryllium armor was determined from the following relationship

$$\kappa=\rho C_p D \qquad (1)$$

where κ is the thermal conductivity, ρ is the density and C_p is the specific heat and D is the thermal diffusivity. A density of 92% of theoretical (1.702 g/cm^3) was used to calculate the thermal conductivity. The specific heat as function of temperature (T) was determined using the following relationship [4]:

$$C_p = 1741.8 + 3.3358 \times T - 3.1125 \times 10^{-3} \times T^2 + 1.2748 \times 10^{-6} \times T^3 \qquad (2)$$

The calculated values for thermal conductivity of the beryllium plasma sprayed armor were then compared directly to the thermal conductivity values for S-65B beryllium [4]. Microstructural characterization of the thermal diffusivity samples was done using polarized and light microscopy after the thermal diffusivity measurements.

The coefficient of thermal expansion (CTE) of the beryllium armor was measured on a quenching and deformation dilatometer manufactured by Materials Measuring Corporation. The beryllium samples were heated in vacuum to 1000 °C and furnace cooled to room temperature. The heating and cooling cycle took approximately 30 minutes to complete. The measured CTE for the beryllium armor was also compared to S-65B CTE data [4].

3. RESULTS AND DISCUSSION

3.1. Chemical Analysis

A chemical analysis of the inert gas atomized beryllium powder used for plasma spraying and the resulting beryllium armor on the CuNiBe and CuCrZr heat sink is given in Table 1. Substantial differences in the chemical analysis between the beryllium powder and the beryllium armor was observed for N, C, BeO, Al and Cu. Increases in the N, C and BeO were attributed to the commercial purity of the processing gases used during the plasma spraying process. The observed increases in the Al and Cu was attributed to erosion of the copper anode inside of the plasma spray torch and erosion of Al parts inside of the powder feeders.

3.2. Four-point bend flexure strength of armor

The flexure strength of the beryllium plasma sprayed armor on the CuNiBe and CuCrZr heat sinks is given in Fig. 4. The stress/displacement curves show a linear strain to failure for the beryllium armor in both cases. The flexure strength of the beryllium armor deposited on the CuNiBe was significantly stronger (~285MPa) then the beryllium which was deposited on the CuCrZr with the aluminum explosive bonded layer (~155 MPa).

Table 1. Chemical analysis of beryllium powder and Be armor material

Element	Be Powder	Be on CuNiBe	Be on CuCrZr
*BeO	.34	.84	.98
*C	.074	.130	.104
Fe (ppm)	920	965	980
Al (ppm)	440	620	625
Si (ppm)	310	405	385
Ni (ppm)	110	105	105
Cu (ppm)	35	115	90
N (ppm)	80	405	395

* wt.%

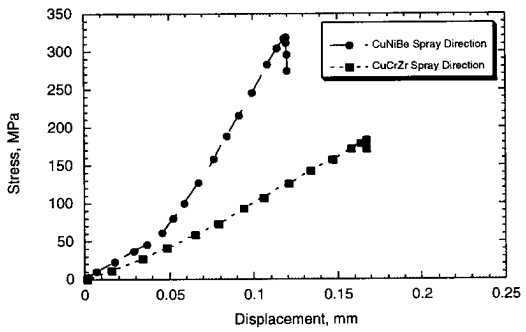

Fig. 4. Results of the 4-point bend flexure strength of the beryllium armor on the CuNiBe and CuCrZr heat sinks.

Strength of plasma sprayed armor is predominately determined by the cohesive strength between the individual splat layers which make up the bulk of the armor. Improvements in the cohesive strength can be accomplished by enhancing the bond between individual splat layers. Microstructural analysis using optical and polarized light microscopy of the beryllium armor on both heat sinks revealed similar microstructural features including porosity striations and unmelted beryllium particles, Fig 5. Immersion densities were also similar and were approximately 92% of theoretical density (1.702 g/cm^3). Transmission electron microscopy studies are currently in progress to determine if their are any significant differences between the inter-splat bonding. The differences in the flexure strength of the beryllium armor is not well understood at this time but may be influenced by differences in the residual stresses that develop during the deposition of the thick beryllium coatings on the two different copper heat sink materials (CuNiBe vs. CuCrZr) and depositing on a copper surface versus depositing on an aluminum surface. In addition, BeO can influence the mechanical strength of beryllium at room and elevated temperatures [5]. Further investigations will need to be performed in order to determine these effects.

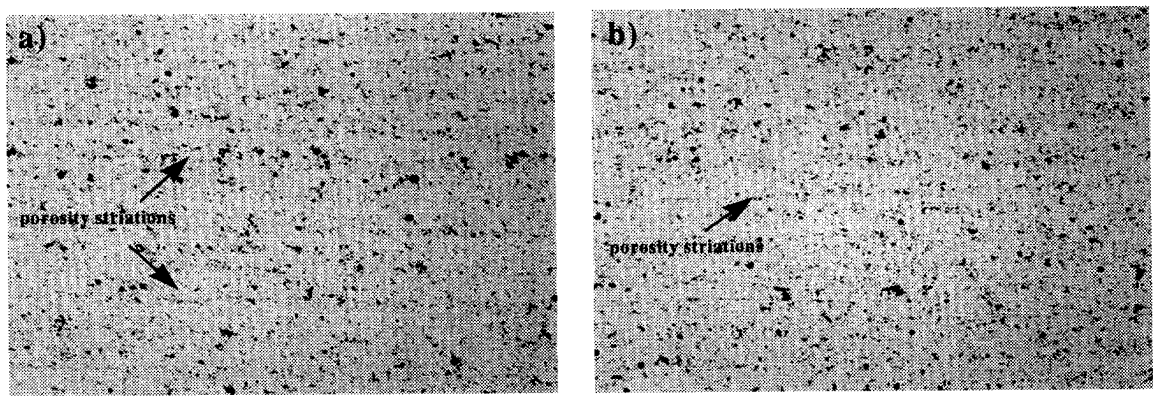

Fig 5. Bright field image of the plasma sprayed beryllium armor a) on the CuNiBe heat sink and b) on the CuCrZr heat sink with an explosive bonded aluminum surface layer. Note porosity striations

3.3. Edge-notched fracture toughness of armor

The stress-displacement curves for the four-point bend edge-notched samples is given in Fig. 6. The maximum stress in bending was approximately 160 MPa for the beryllium armor on the CuNiBe and CuCrZr heat sinks. The two samples exhibited similar stress-displacement behaviors during four-point loading. There was an initial load increase followed by load leveling. Beyond a critical displacement the load increased until sample failure had occurred.

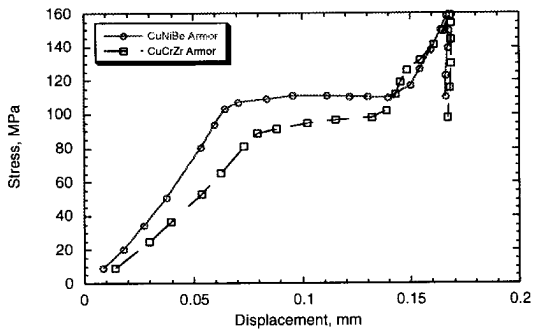

Fig. 6. Stress-displacement plots for edge-notched four-point bend testing of the beryllium armor.

A constant load with an increase in displacement is typically observed in materials which exhibit R-Curve behavior [6]. R-curves characterize the resistance to fracture of a material during crack extension. The constant load and increase crack extension represents a "pop-in" effect which arises from a sudden unstable, rapid crack propagation before the crack slows down to a more stable crack advancement. In the plasma sprayed beryllium armor, porosity striations were observed throughout the coating thickness and can potentially influence the crack advancement through the armor. The fracture toughness, K_{1C}, for the beryllium armor on the CuNiBe was approximately 9.26 MPa $m^{1/2}$ and 8.56 MPa $m^{1/2}$ for the beryllium armor on the CuCrZr heat sink with an explosive bonded aluminum surface layer. The presence of porosity in beryllium has been shown to improve the fracture toughness of beryllium [6].

3.4. Interfacial strength of Be armor/heat sink

The stress-displacement results from a four point bend test to determine the interfacial strength between the plasma sprayed beryllium armor on the CuNiBe heat sink and the CuCrZr heat sink with aluminum explosively bonded to the surface are shown in Fig. 7.

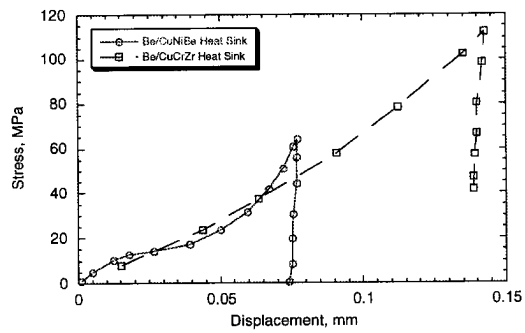

Fig. 7. Four-point bend strength of the interface between the beryllium armor on the CuNiBe heat sink and on the CuCrZr heat sink.

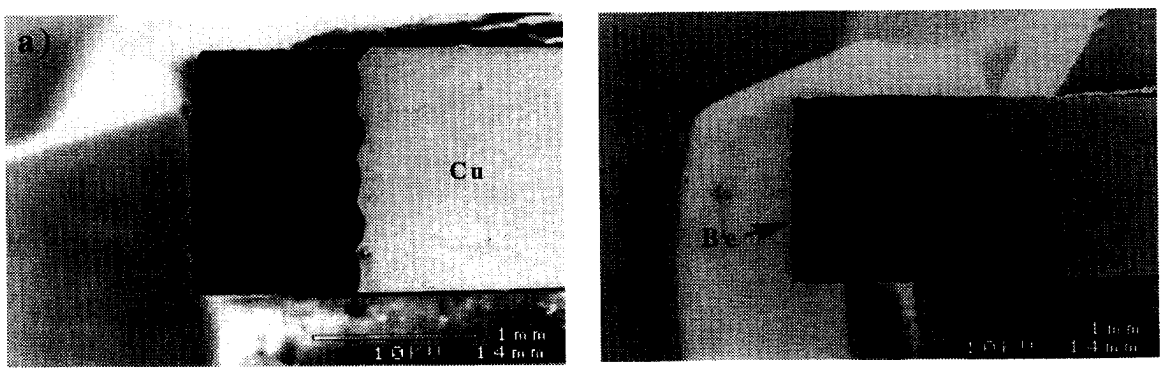

Fig. 8. Location of the failure in the beryllium armor during the four-point bend interfacial strength test. A) beryllium armor on CuNiBe heat sink and b) beryllium armor on the CuCrZr heat sink with an explosive bonded aluminum surface layer.

In both cases, failure occurred in the beryllium armor and not at the beryllium/heat sink interface during the four-point bend test, Fig 8. The strength of the beryllium armor on the CuNiBe heat sink (~70 MPa) was significantly lower than the strength of the beryllium armor on the CuCrZr heat sink (~110 MPa). Failure typically initiated in the beryllium armor and propagated along a path parallel to the heat sink interfaces. Cracking parallel to the interface is often seen in joints of dissimilar materials like ceramic/metal systems [7-9]. The thermal expansion mismatch between dissimilar materials can result in compressive stresses at the interface causing a crack to be deflected away from the interface, but still travel parallel to the interface. The plasticity and relative toughness of the interface along with residual tensile stresses in the plasma sprayed beryllium armor can promote cracking in the beryllium armor at coating defects. The interfacial strength between the beryllium armor/ heat sink was stronger, in both cases, than the beryllium armor itself.

3.5 Ultrasonic C-scan results of beryllium armor/heat sink interface

Baseline ultrasonic C-scans of the interface between the 5 and 10 mm beryllium armor tiles on the CuNiBe and the CuCrZr heat sinks are given in Figs 9 and 10. These preliminary ultrasonic C-scans were done to determine the relative bond quality of the beryllium armor to the heat sink materials before high heat flux testing. The squares in the ultrasonic C-scans represent the individual beryllium tiles on the Be/Cu mockups. A dark region in the ultrasonic C-scan indicates a high intensity spot where a potential defect/discontinuity at the interface existed. The low intensity ultrasonic C-scans for the beryllium armor on the CuNiBe and CuCrZr heat sinks was an indication of no appreciable defects at the armor/heat sink interface.

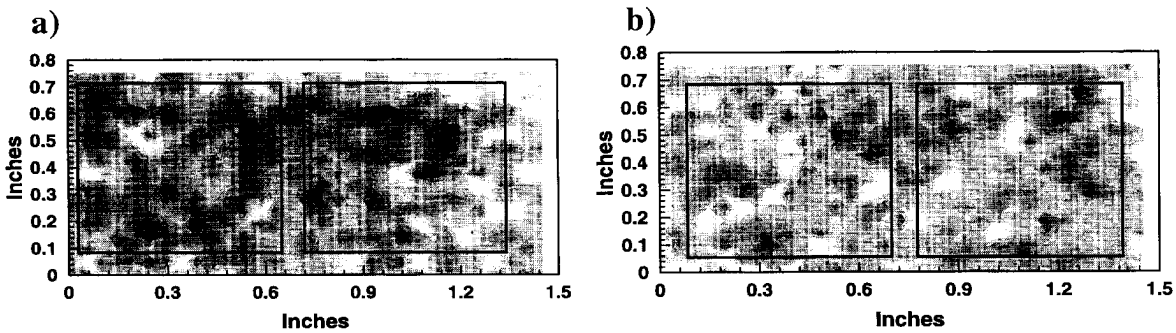

Fig. 9. Benchmark ultrasonic C-scan of interface of Be on CuNiBe heat sink. The sample contains two 5-mm tiles (a) and two 10-mm tiles (b). The squares represent the boundaries of the armor tiles

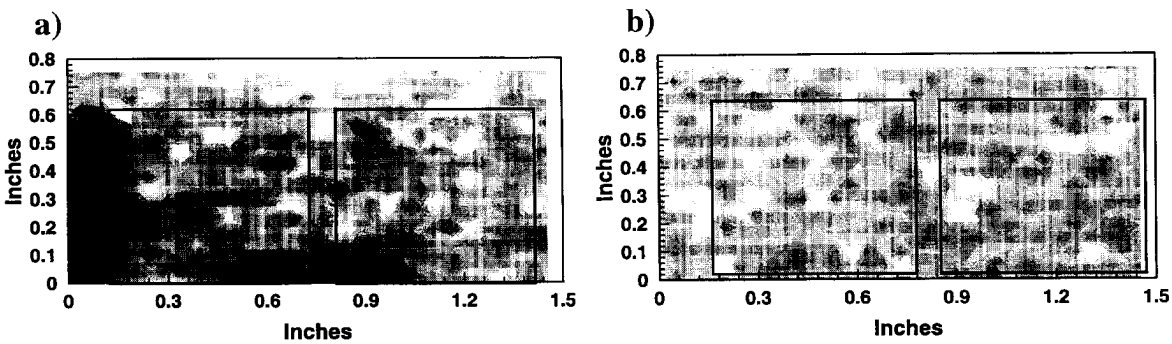

Fig 10. Benchmark ultrasonic C-scan of interface of the Be armor on a CuCrZr heat sink with an explosive bonded aluminum surface layer. The sample contains two 5 mm tiles (a) and two 10 mm tiles (b). The squares represent the boundaries of the armor tiles.

In the case of the beryllium armor on the CuCrZr heat sink, Fig. 10, the ultrasonic C-scan did indicate a region of high intensity on the lower portion of each of the 5 mm tiles. Although the spots indicated localized areas of poor bond quality, we suspected the damages were caused by drilling of thermocouple holes in the copper heat sink and the beryllium tiles.

3.6. Thermal expansion of beryllium armor

Thermal expansion through the thickness of the beryllium armor (*i.e.*, in the spray direction) and in the plane of the armor (*i.e.*, normal to the spray direction) is given in Fig.11. The CTE for both orientations had a behavior similar to S65-B from room temperature to 400 °C. A slight anisotropy in CTE was observed for the two orientations. Above 400 °C the plasma sprayed beryllium armor showed a significant contraction for both orientations. This behavior has been previously observed in plasma sprayed beryllium and has been attributed to microstructural effects in the plasma sprayed beryllium coating [10].

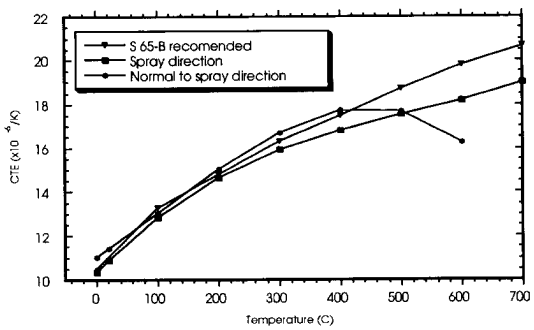

Fig. 11. Thermal expansion through the thickness of the beryllium armor (i.e., in the spray direction) and in the plane of the armor (i.e., normal to the spray direction)

Under an applied load at elevated temperatures the layered microstructure, which is typically seen in plasma sprayed coatings, can slide against each other producing the observed contraction. The amount of contraction can vary depending upon the bond strength between individual splat layers. At higher temperatures and applied loads the contraction due to sliding can potentially lead to densification of the beryllium plasma sprayed coating. The differences in the CTE between the armor tested through the thickness of the coating and along the plane of the coating can be attributed to the difference in orientation of individual splat layers and the effective resistance to sliding.

3.7. Thermal conductivity of beryllium armor

A comparison of the through thickness thermal conductivity from room temperature to 600 °C for beryllium plasma sprayed armor on the CuNiBe and the CuCrZr heat sink is shown in Fig 12. and compared to S65-B beryllium.

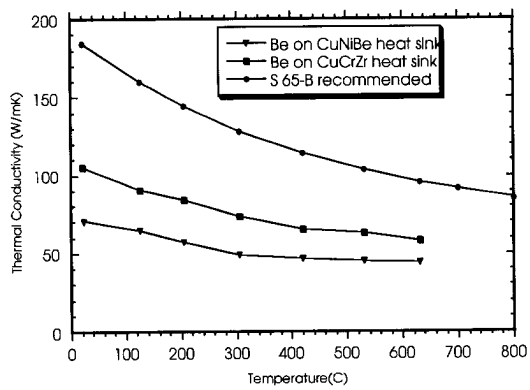

Fig. 12. A comparison of the through thickness thermal conductivity from room temperature to 600 °C for the beryllium plasma sprayed armor on the CuNiBe and the CuCrZr heat sink. Results are compared to S65-B.

The thermal conductivity of the beryllium deposited on the CuNiBe heat sink was approximately 40-50% of S65-B over the room temperature to 600°C temperature range whereas the thermal conductivity of the beryllium deposited on the CuCrZr heat sink, which had an explosive bonded aluminum surface layer, was approximately 60-70% of S65-B. Both beryllium armor samples showed a similar trend in thermal conductivity to S65-B from room temperature to 600 °C. The microstructure, Fig 5, and immersion density (approximately 92% of theoretical) of the beryllium armor samples were similar and showed no obvious differences. In both cases, porosity striations were observed throughout the thickness of the beryllium coating. Although the difference between the thermal conductivity of the beryllium armor is not fully understood, a number of factors such as pore size and pore distribution [11], splat-to-splat cohesion within the coating [12] and the amount and distribution of BeO in beryllium [10] may contribute to the observed differences.

The residual stresses during the deposition and build-up of the thick beryllium armor may also influence both the mechanical and thermal properties of the final beryllium coating. Further investigations are needed in order to evaluate the contribution of these various factors.

An anisotropy in thermal conductivity was observed in the plasma sprayed beryllium armor, Fig 13. The thermal conductivity in the spray direction was lower than the thermal conductivity normal to the spray direction over the room temperature to 600°C temperature range.

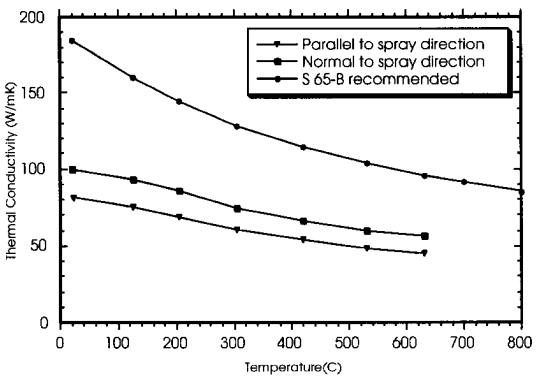

Fig. 13. A comparison of the thermal conductivity through the thickness of the beryllium armor (i.e., in the spray direction) versus in the plane (i.e. normal to the spray direction) of the beryllium armor.

This difference in conductivity can also be attributed to microstructural effects of the plasma sprayed beryllium armor which consists of individual molten particles which impact and spread into individual splat layers building-up the thickness of the coating. Layer separation between individual splats can result in a thermal resistance across the splat interfaces which can reduce the through thickness thermal conductivity [12]. The presence of the porosity striations which are normal to the through thickness of the coating and in the heat conduction path, can also provide a thermal resistance at each striation. Porosity striations along the length of the heat conduction path, which were present in the samples tested in the plane of the coating, would not provide as much resistance to thermal conduction.

4. CONCLUSION

Be/Cu mockups for high heat flux testing were produced by plasma spraying beryllium on heat sink materials of CuNiBe and CuCrZr with an explosive bonded layer of aluminum. Characterization of the thermal and mechanical properties of the plasma sprayed beryllium armor and the interface between the armor and the heat sink material was performed prior to the high heat flux testing. In general, both the thermal and mechanical properties where effected by the microstructural development of the plasma sprayed beryllium armor. The layered structure which is produced from the individual splats which make up the bulk of the beryllium armor contributed to differences in the thermal expansion, thermal conductivity, flexure strength and fracture toughness of the beryllium armor. Other factors such as the oxide content, residual stress and splat-to-splat cohesion may also have contributed to the observed differences in the thermal and mechanical properties. Further investigations will need to be performed in order to evaluate the contributions of each of these factors.

ACKNOWLEGEMENTS

The authors would like to acknowledge the following people for their contributions: Dr. D.P.H. Hassleman of Virginia Polytechnic Institute for thermal diffusivity measurements, Dr. D.J. Thoma for thermal expansion measurements, metallography and powder characterization laboratory's at LANL for sample preparation and characterization, Brush Wellman Inc. for chemical analysis and Karta Technology for ultrasonic C-scan testing. This research was sponsored by the DOE Office of Fusion Energy.

REFERENCES

1. Cadden and B.C. Odegard, Jr., "Aluminum-Assisted Joining of Beryllium to Copper for Fusion Applications", Sandia National Laboratories Report SAND97-8445, Jan., 1997.
2. R.G. Castro, K.E. Elliott, R.D. Watson, D.L. Youchison and K.T. Slattery, "Fabrication and High Heat Flux Testing of Plasma Sprayed Beryllium ITER First Wall Mock-ups," Proceedings on the Inter. Conf. on Fusion

Reactor Matls., ICFRM-8, Sendai, Japan, October 27-31, 1997.

3. R.P Tye, Thermal Conductivity, Vol 2, Academic Press Inc., New York 1969, p. 191-197.
4. V. Varabash, "Recommended Data on Be Thermomechanical Properties for Plasma Facing Components: Design Evaluation" ITER Draft Report NG1, ITER Garching Joint Work Site, (1994) p. 7-8.
5. D.R. Floyd and J.N. Lowe., Beryllium Science and Technology, Plenum Press, New York 1979.
6. G.E. Dieter, Mechanical Metallurgy, 3rd edition, McGraw-Hill Company (1986) p. 348
7. M. D. Drory and A. G. Evans, J. Am. Ceram. Soc., 73 (1990) 634.
8. A. H. Bartlett, A. G. Evans, and M. Ruhle, Acta Metall. Mater., 39 (1991) 1579.
9. S. D. Conzone, D. P. Butt, and A. H. Bartlett, J. Mater. Sci., 32 (1997) 3369.
10. D.R. Floyd and J.N. Lowe., Beryllium Science and Technology, Plenum Press, New York 1979, p. 135-173.
11. K.J. Hollis, Ph.D. Thesis, University of Wisconsin-Madison (1995).
12. R.G. Castro, P.W. Stanek, K.E. Elliott, J.D. Cotton and R.D. Watson, J. Nucl. Mater. 226 (1996), 77-83.

DISCLAIMER

Report Number (14) LA-UR--97-4201
CONF-970153--

Publ. Date (11) 199712
Sponsor Code (18) DOE/ER, XF
UC Category (19) UC-424, DOE/ER

DOE